

Fiber-Based Modeling for Investigating the Effect of Load History on the Behavior of RC Bridge Columns

Y. Feng, M.J. Kowalsky & J.M. Nau

North Carolina State University, Raleigh



SUMMARY:

Ensuring that structures achieve their desired performance level under a prescribed seismic event is the goal of performance based design. The prediction of performance requires accurate models to define damage, which are often characterized on the basis of strain, and accurate methods to correlate strain to structural deformations. Given the variability in ground motion characteristics, it is of obvious importance to understand any potential impact that loading history may play in the prediction of performance. To that end, this paper discusses the development, calibration, and application of a fiber-based model that is ultimately used to conduct a detailed parametric study on the effect of seismic loading history on the behavior of reinforced concrete bridge columns. The goal of calibration is to ensure that the model can capture both structural level behavior, which includes global force-displacement response, and material and section level behavior, such as strain and curvatures.

Keywords: fiber, reinforced concrete, load history

1. INTRODUCTION AND BACKGROUND

The goal of performance based earthquake engineering is to design a structure to achieve a prescribed performance level under a prescribed seismic event. To accomplish this, a reliable model is required to characterize performance, which is usually defined on the basis of strain, and its correlation with structural deformation. Given the variability in ground motion characteristics, it is of obvious importance to understand any potential impact that loading history may have on the structural behavior. For this purpose, a research program is ongoing on load history effects at North Carolina State University which consists of extensive large scale tests on reinforced concrete bridge columns and analytical studies using fiber and finite element methods. Fiber-based modeling utilizes the Open System of Earthquake Engineering Simulation (OpenSees) which is an open-source platform to simulate the behavior of structures under seismic loading.

This paper discusses the development and calibration of the fiber-based model. The goal of calibration is to ensure that the model can capture both structural level behavior, which includes global force-deformation response, and material or section level behavior, such as strain and curvature levels. The application of this fiber model is also introduced which includes an ongoing parametric study of the load history effect on both the strain deformation relationship and on the strain limits themselves. The study of the load history effect on strain limits also involves a finite element model for predicting buckling of reinforcement, which represents a common seismic damage mechanism in well-detailed reinforced concrete structures. Predictions of force-deformation and strain hysteretic response are compared to data from experimental tests. In addition, responses from two shake table tests are also utilized to verify the dynamic performance of the fiber model.

A series of eighteen columns have been tested to date at NCSU as the experimental portion of the load history project. The large scale columns were subjected to 3-cycle-set loading history as well as earthquake load histories. The experimental observations have been discussed by Goodnight et al.

(2012). An optical 3D measurement system (Optotrak) was utilized to obtain the engineering strain in the longitudinal reinforcement. A series of LED markers were attached to the exposed reinforcement and the sensors captured the movement of the LED markers in the 3D space. The elongation of the distance between two LED markers was utilized to calculate the average strain in each gauge length. This technique provides strain histories along the longitudinal direction of the bar. However, there are two basic assumptions on the strain calculation with Optotrak data that the reinforcement behaves uniaxially and the localization of strain doesn't occur inside one gauge length. Therefore, the strain calculated from Optotrak data are considered to be valid before bar buckling or necking. The Optotrak system and its operating mechanism are displayed in Fig. 1.

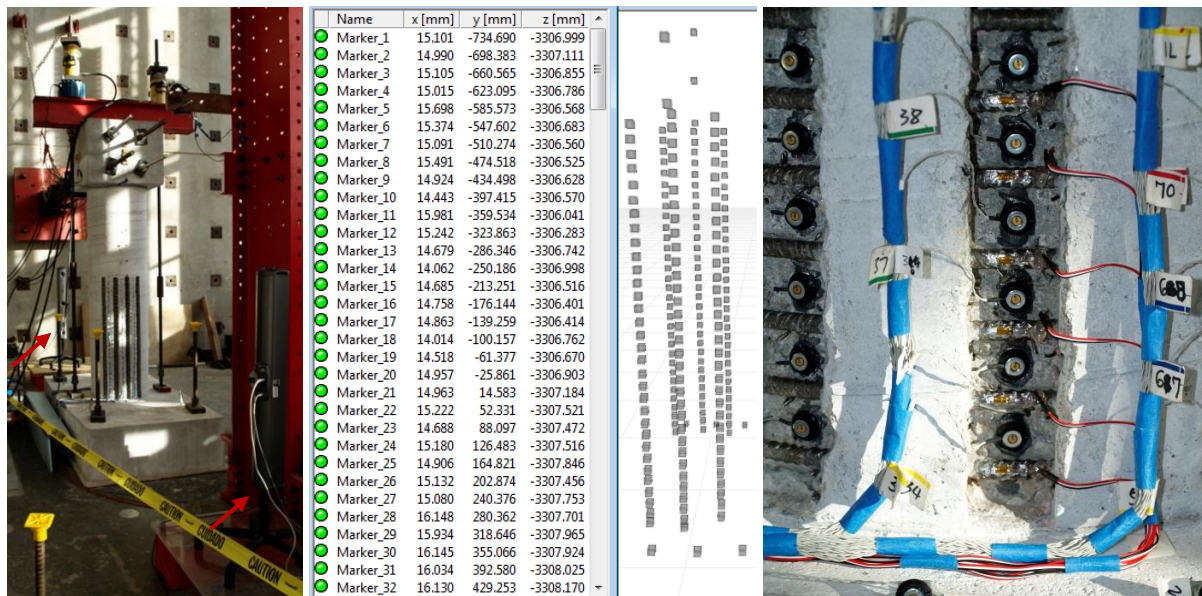


Figure 1. The dual camera Optotrak system, coordinate system, and LED markers on the reinforcement

2. UNIAXIAL MATERIAL AND FIBER SECTION

In fiber-based models, materials have only uni-directional strength and stiffness whose behavior is defined in terms of its stress-strain response. For the convenience of users, OpenSees provides a number of constitutive models for each type of material. These constitutive models were developed by various researchers into this open-source software. A few parameters, such as steel yield strength and concrete compressive strength, are usually required to define both monotonic and cyclic stress-strain behavior. This research selected the steel model developed by Filippou, et al. (1983) and the concrete model developed by Yassin (1994) for analysis. The steel material allows the user to control the cyclic behavior by defining a pair of isotropic hardening ratios in addition to adjustable yield strength and elastic modulus. The concrete constitutive model has an inherent cyclic behavior which depends on the user defined strength parameters.

Fiber sections are assumed to remain plane throughout the analysis. In reinforced concrete structures, the fiber section is assembled with pre-defined concrete and steel materials. The section is divided into a number of concrete patches where the steel fiber will be located. Strain compatibility between reinforcement and surrounding concrete is assumed. The sectional reactions under force and moment are in terms of axial strain at mid-section and curvature. A unique solution of this deformation combination will be obtained based on the moment-curvature analysis of the section.

3. BEAM AND COLUMN ELEMENTS IN THE FIBER MODEL

The integration scheme plays a significant role in a fiber-based element. It determines the locations of integration points where fiber sections are placed. In addition, the integration scheme is utilized to obtain either the global stiffness or flexibility matrix along with the interpolation function of displacement or force. The type of the integration scheme and the number of integration points determine the order of exact integration. Various integration schemes are available in elements, including the Gauss-Lobatto, Gauss-Legendre, Gauss-Radau integration.

Two major types of fiber-based elements in OpenSees are the displacement-based element and the force-based element (flexibility-based element). The displacement-based element utilizes a displacement interpolation function to distribute the nodal deformation along the element length. The nodal force is related to sectional behavior by integrating the sectional stress along with the interpolation function. Equilibrium is satisfied in a weighted integral sense as expressed in Eqn. 1.1 from Alemdar and White (2005).

$$\int_0^L \mathbf{N}(x)^T \mathbf{D} dx - \mathbf{Q} = \mathbf{0} \quad (1.1)$$

$\mathbf{N}(x)$ is constructed with the displacement interpolation functions. Matrix \mathbf{D} is the stress-resultant section force. \mathbf{Q} is the external force at nodes and L is the length of the element. Neuenhofer and Filippou (1998) proposed a force-based element where a prescribed force field is assigned instead of the displacement interpolation function. It adapted a governing compatibility equation derived from the principle of virtual work as shown in Eqn. 1.2.

$$\int_0^L \mathbf{N}_F(x)^T \mathbf{d} dx - \mathbf{q} = \mathbf{0} \quad (1.2)$$

$\mathbf{N}_F(x)$ represents the force interpolation functions. The sectional strain is represented by \mathbf{d} . The matrix \mathbf{q} is referred to as the nodal displacement. Curvature-Based Displacement Interpolation (CDBI) was used to account for geometric nonlinear effects. At a coarse mesh level, the CDBI method ensures that the distribution of deformation has a relatively high order of accuracy.

The force-based element satisfies equilibrium strictly on a section-by-section basis. On the other hand, the displacement-based element satisfies equilibrium in a weighted integral sense at element nodes only. The imposed displacement field is an assumption which may not capture the real behavior in structural components. To compensate for this potential shortcoming, a fine mesh is usually required for the displacement-based element thus increasing the computational cost.

The force-based element, however, suffers from strain-softening behavior which results in the loss of objective. The reinforced concrete section in fiber models tends to have strain-softening behavior because of the post-peak softening of concrete. The force field in the element causes the maximum moment to always be located at the same critical section. In the extreme load case, the critical section may deform to pass the peak capacity point which prevents other sections from reaching their peak capacity. Consequently, the deformation will concentrate at the integration point associated with the critical section. The computed response is determined by the spread of this concentrated deformation implied by the integration weight. As a result, a unique solution does not exist and it is mesh dependant. In other words, the force-based element sacrifices the inter-sectional compatibility to enforce the inter-sectional equilibrium. There is no compatibility restriction on the deformation gradient between two adjacent sections.

A special type of force-based element was developed by M. Scott and F. Fenves (2006) to overcome the loss of objective problem. The ‘beam with hinges’ element utilizes a plastic hinge integration method which allows defining the integration weight of the critical section with a plastic hinge length.

The element involves a modified Gauss-Radau integration rule where the weight of the end integration point is adjustable. Though the regular force-based element allows user to alter the weight of the end integration point to accomplish the same goal, the length of the weight cannot be defined to the pre-calculated plastic hinge length since it depends on the number of integration points. The ‘beam with hinges’ element is more convenient for reconciling the integration weight to a plastic hinge length. To reduce the computational cost, an elastic region is defined at the interior portion of the ‘beam with hinges’ element. The elastic properties, such as elastic modulus, area and moment of inertia, are required at the interior region. It has been observed in the experimental tests that cracked regions cover most of the reinforced concrete column. As a result, a cracked section moment of inertia was used to model the elastic portion of the element.

To evaluate the accuracy of both the ‘beam with hinges’ element and the displacement-based element, the analytical results are compared to test data. The experiments include a series of cyclic column tests with 3-cycle-set load history and earthquake load histories. The reinforced concrete columns are 8 ft (2.44m) high and 2 ft (0.61m) in diameter. The reinforcement content is 16 0.75 in (19mm) diameter bars and 0.375 in (9.5mm) spiral at 2 in (51mm) pitch. As shown in Fig. 1, the ‘beam with hinges’ element generates a better prediction of the force-deformation relationship for the 3-cycle-set test result. It is also observed in other analysis that the displacement-based element tends to overpredict the strength of the specimen. Though a finer mesh can improve accuracy of displacement-based element, difficulty with convergence may occur in the analysis. As a result, the ‘beam with hinges’ element is shown to be better at capturing the behavior of reinforced concrete columns, and was therefore selected for subsequent calibrations.

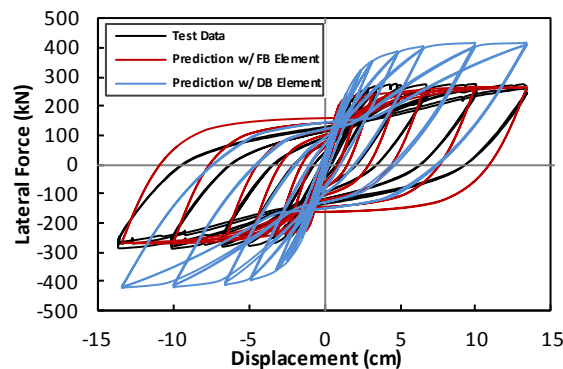


Figure 1. Comparison between model predictions and test data

4. STRAIN PENETRATION MODEL

It is illustrated in Fig. 2 that cracking was observed on the footing surface. When the column is subjected to large flexural deformation, a crack initiated near the tensile side of the column. This is due to the strain penetration of the longitudinal reinforcement into the footing. As the longitudinal reinforcement has large tensile strains in the plastic hinge region, a strain gradient is required inside the footing to allow the reinforcement strain to reduce to zero. Globally, the reinforcement will slip from footing to a certain amount of displacement which depends on the strain gradient level in the footing. A small portion of the footing surface concrete, which is bonded to the reinforcement, cracks to accommodate this bond slip displacement.

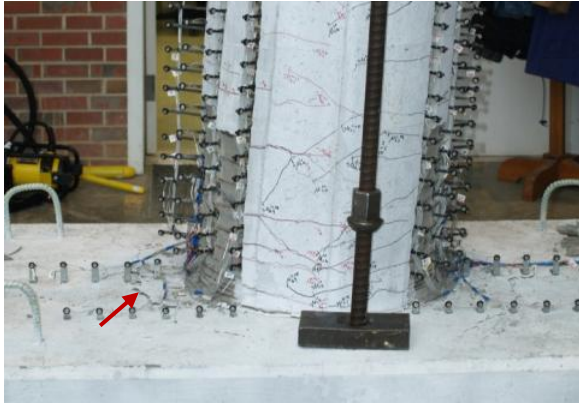


Figure 2. Crack on the footing near the tension side of the column

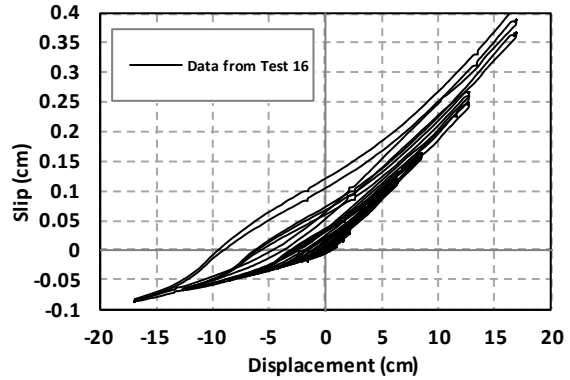


Figure 3. Bond slip hysteretic response

In experimental tests, the bond slip displacement of reinforcement can be obtained by monitoring the vertical movement of the LED markers. Fig. 3 portrays the bond slip hysteretic response at the lowest marker level on the reinforcement. Since the monitored marker is located about 1.0 in (25.4mm) above the footing surface, the bond slip displacement may include a portion of plastic elongation of the reinforcement. This elongation could not be quantified precisely without the strain data at this location of reinforcement. However, Fig. 3 still demonstrates the general behavior of bond slip.

A zero length section element is located at the base of the column element to include the bond slip behavior, as presented in Fig. 4. The zero length element serves as a nonlinear rotational spring which accounts for the additional rotation at the base column section due to bond slip. The behavior of the zero length element depends on the associated fiber section. The fiber section consists of concrete fiber and reinforcement fiber which is represented by a bond slip material. Zhao and Sritharan (2007) developed a bond slip material which implemented a stress-slip relationship to account for the strain penetration. The bond slip is represented by the slip displacement in the material which depends on the stress in the reinforcement, as shown in Fig. 5.

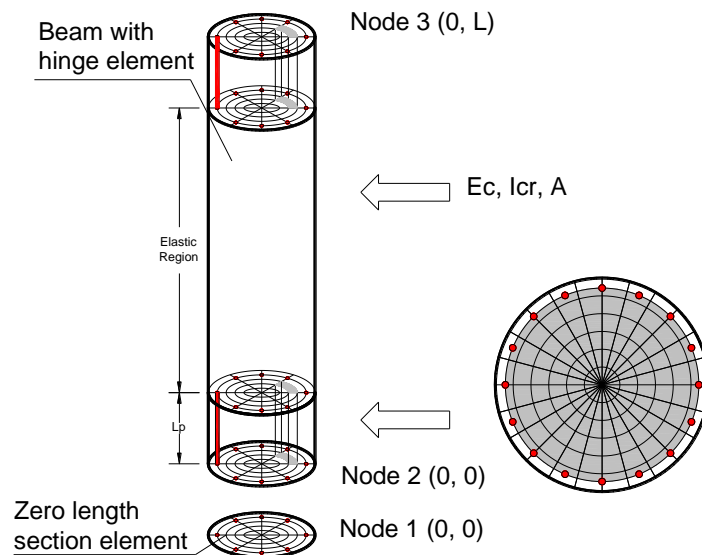


Figure 4. Lay-out of fiber model

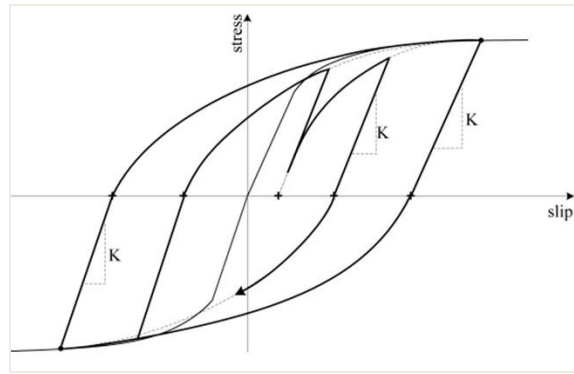


Figure 5. Stress-slip relationship from Zhao and Sritharan (2007)

5. CALIBRATION OF THE FIBER MODEL WITH TEST DATA

The fiber model was calibrated with recorded data from different types of experiments, such as material testing, large-scale static column testing, and shake table tests. A robust model should have the capacity to predict the force-deformation response, strain, and dynamic response. Nevertheless, concrete cracking, reinforcement bar buckling and rupture cannot be simulated with fiber-based models. Cracking of concrete causes a localized discontinuity in the material which violates the uniform deformation scenario in the fiber-based element. The buckling and rupture of reinforcement are multi-dimensional nonlinear behaviors which the uniaxial material fails to model. As a consequence, the calibration discussed below will not capture these behaviors.

5.1. Calibration on Material Constitutive Models

A number of bar cyclic tests were conducted to ensure proper steel material behavior modeling. The constitutive material model was adjusted to match the bar test result which is shown in Fig. 6. The concrete compression strength was obtained from cylinder tests. The monotonic behavior of confined concrete was derived with the stress-strain model proposed by Mander et al. (1988). The concrete cyclic behavior is controlled by the constitutive model in OpenSees, as presented in Fig. 7. Tension strength of concrete was neglected in the model.

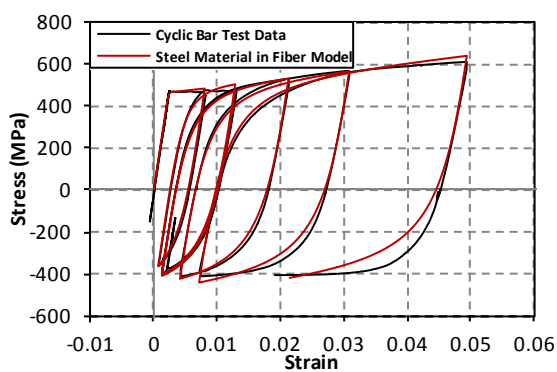


Figure 6. Comparison between behavior of steel material in fiber model and test data

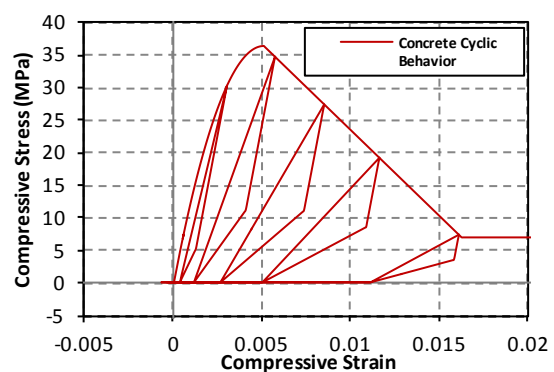


Figure 7. Concrete cyclic behavior in fiber model

5.2. Calibration with Data from Static Tests

The fiber model is evaluated with the complete data set from the eighteen column tests where the strain information is available up to reinforcement buckling. It is observed that the behavior of the zero length section element and the numerical plastic hinge length have a large impact on the strain

prediction. As a result, calibration concentrates on these two areas.

With the proposed cyclic bond slip behavior, the zero length element has relatively low moment capacity compared to the column section. It results in a strain-softening behavior where deformation concentrates in the bond slip model in terms of rotation. Consequently, the fiber model underestimated curvature and the resultant strain at the base section of the column element. The moment capacity of the bond slip model was enhanced to overcome the problem. The proposed bond slip model suggests defining the ultimate slip at maximum stress of reinforcement to be 30 to 40 times the slip at yield stress. By decreasing the ultimate slip level, the zero length section element has a higher strength which migrates a portion of the rotational deformation to the column base section.

The plastic hinge length controls the extent of plasticity in the ‘beam with hinges’ element. The plastic hinge length can be specified by an empirical relationship proposed by Priestley et al. (2007), as shown in Eqn. 5.2.1 to 5.2.3

$$L_{SP} = 0.022 f_y d_{bl} \tag{5.2.1}$$

$$k = 0.2 \left(\frac{f_u}{f_y} - 1 \right) \leq 0.08 \tag{5.2.2}$$

$$L_P = kL_C + L_{SP} \geq 2L_{SP} \tag{5.2.3}$$

where L_{SP} , L_P and L_C are the strain penetration length, the plastic hinge length, and the column length, f_y , f_u and d_{bl} are yield strength in MPa, ultimate stress in MPa and diameter of longitudinal reinforcement in millimetre respectively.

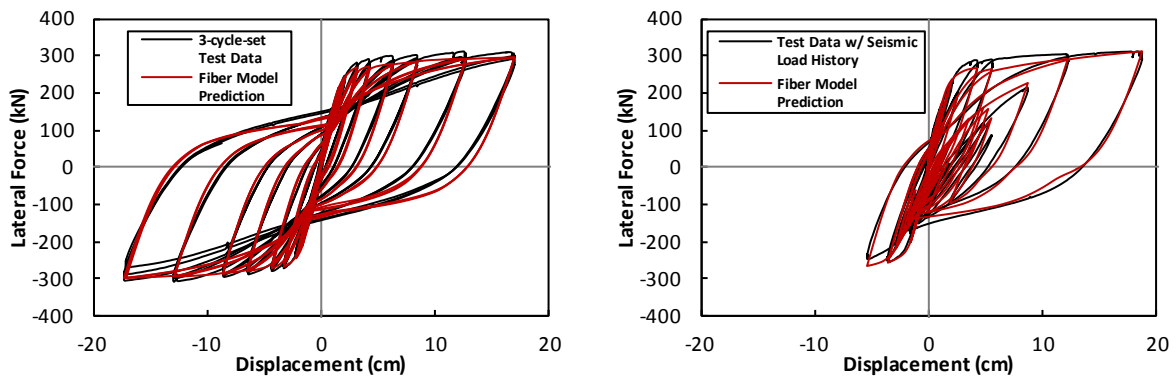


Figure 8. Comparison of force-deformation responses from the fiber model and test data

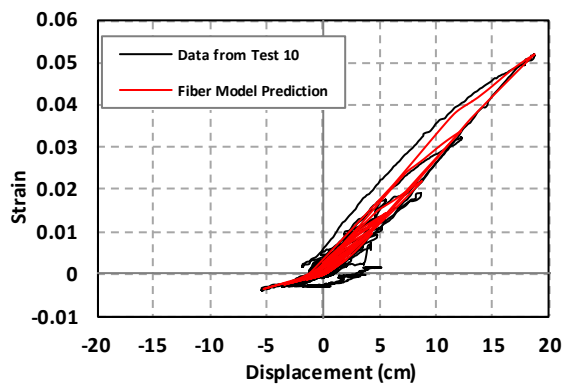


Figure 9. Comparison of strain hysteretic response from the fiber model and test data

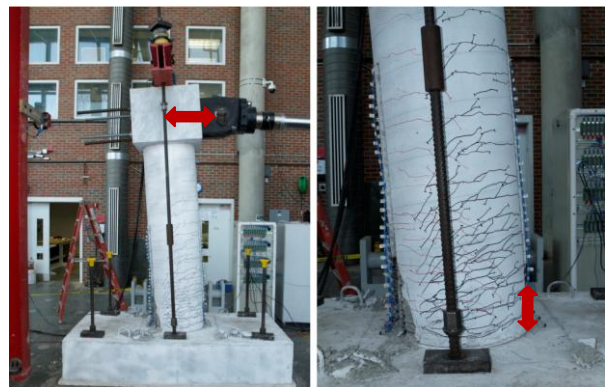


Figure 10. Locations of displacement measurement and associated strain measurement (red arrow)

Fig. 8 demonstrates the comparison of force-deformation responses between the fiber model and test data with a 3-cycle-set load history and earthquake load history. The section-by-section-based equilibrium in the force-based element ensured an accurate prediction of response. The bond slip model contributes to the proper unloading and reloading stiffness of the model. However, the cycle to cycle strength degradation in the 3-cycle-set loading pattern is not captured because of the absence of cycle to cycle relaxation behavior in the steel constitutive model and cumulative damage in concrete. The strain hysteretic response in Fig. 9 represents the relationship between the structural deformation and the local strain which indicates the damage in the plastic hinge region. As shown in Fig. 10, the top column displacement is measured as the structural deformation and the strain is obtained from the plastic hinge region. The comparison shows good agreement between the model prediction and test data, especially, at the peak strain level. However, the residual strain at zero displacement level is consistently underestimated by the fiber model. Therefore, the accumulation of reinforcement strain over multiple cycles is not captured precisely. The solution to overcome this shortage could be developing an advanced reinforcement material model to include the low cycle fatigue behavior of steel since most of current constitutive models are calibrated with material testing with limited cycles.

5.3. Calibration with Data from Shake Table Tests

The dynamic performance of the fiber model is important for the future parametric study which is based on nonlinear time history analysis. For the purpose of estimating the dynamic performance, the fiber model was implemented to predict the displacement response of two shake-table tests. In fiber-based time history analysis, Petrini et al. (2008) presented that no additional damping should be added for structural representation in a fiber model, since the hysteretic damping has been included at the material level. Therefore, there is no viscous damping applied to the fiber model.

Petrini et al. (2008) generated the first shake-table test at Centre of Research and Graduate Studies in Earthquake Engineering and Engineering Seismology (ROSE school) where a hollow reinforced concrete column was subjected to Morgan Hill earthquake. Pacific Earthquake Engineering Research Centre (PEER) and Network for Earthquake Engineering Simulation (NEES) sponsored the Concrete Column Blind Prediction Contest (2010) at University of California, San Diego (UCSD). A full scale reinforced concrete bridge column was tested under a series of six ground motions from Loma Prieta earthquake (1989) and Kobe earthquake (1995). The comparison between the displacement responses from fiber model and the ones from the shake table tests are shown in Fig. 11. The fiber model captures most of the major peaks in the displacement response, however, underestimates the residual displacement by a small amount. In the UCSD shake table test, the small amount of underestimation on residual displacement is due to lack of representation on cumulative damage in concrete. The extensive large residual displacement in the shake table test at ROSE school is likely a result of local damage in the plastic hinge region, such as reinforcement buckling and concrete crushing or spalling. This column also ultimately suffered collapse due to a large P-Delta moment.

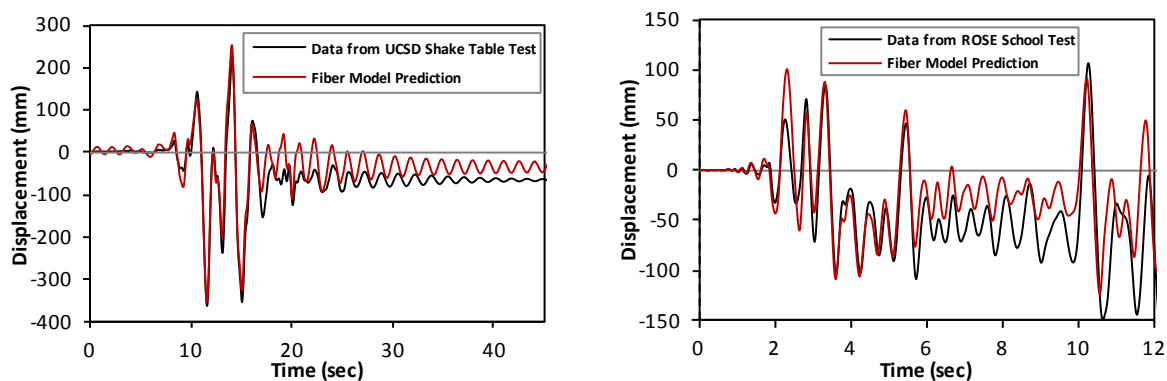


Figure 11. Comparisons of displacement response from fiber model and test data

It has been presented in the comparisons that the fiber model is able to predict accurate force-deformation response and strain hysteretic response of reinforced concrete columns. Also, time history

analyses with fiber models are able to predict dynamic response.

6. INTRODUCTION OF PARAMETRIC STUDY ON LOAD HISTORY EFFECT

As discussed before, load history may impact strain limit state definition and the relationship between displacement and strain. This parametric study will focus on strain limits defined by buckling of reinforcement. As a multi-dimensional mechanism, buckling cannot be captured by the uniaxial fiber model. The fiber model can only include the influence of buckling in force-deformation response by incorporating pre-defined buckling stress-strain behavior in the reinforcement constitutive model. However, with its ability to predict the strain hysteretic response, fiber-based modeling can be utilized to study the effect of load history on the relationship between strain and displacement. Variables in the parametric study include aspect ratio, axial load ratio, bar diameter, as well as transverse reinforcement detailing. By altering one variable at a time, the column models were subjected to multiple earthquakes respectively, and the load history effect on the strain displacement relationship characterized. A couple of example comparisons on strain hysteretic response are presented in Fig. 12.

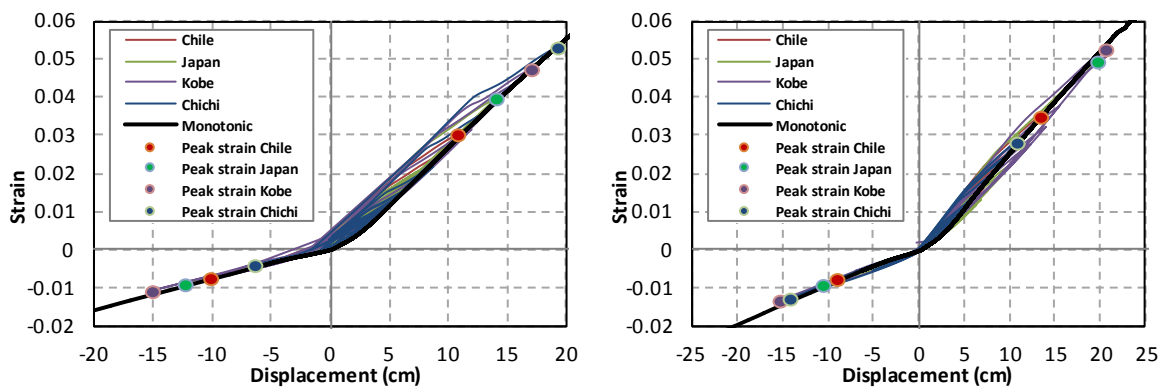


Figure 12. Comparison between strain hysteretic responses with 5% (left) and 10% (right) axial load ratio

The finite element analysis program Abaqus was used to simulate the buckling mechanism of reinforcement. Initially, the entire column was modeled with reinforcement elements embedded in the concrete matrix. The highly nonlinear behavior at the plastic hinge region prevents most of the analysis from converging. The computational cost is tremendous with the complicated concrete model from plasticity theory. An alternative method is proposed here in which a portion of the reinforcement as well as the boundary condition in the plastic hinge region are simulated, as shown in Fig. 13. A series of axial displacements are imposed on the model to duplicate the strain history predicted by the fiber model. Calibration is ongoing for improvement of the accuracy on capturing the strain history effect on buckling. This “combined” methodology will be adapted for future parametric studies of the load history effect on strain limits defined by buckling of reinforcement.

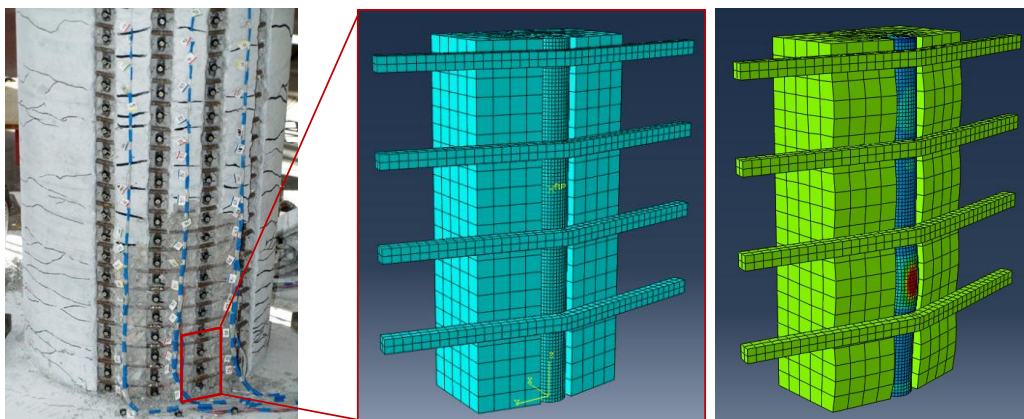


Figure 13. Modeling of local area of column and buckling of reinforcement captured

7. CONCLUSION

The force-based element in the fiber model provides an accurate prediction of force-deformation response of reinforced concrete bridge columns. The 'beam with hinges' element defines the extent of plasticity and overcomes the loss of objective caused by strain-softening behavior. A zero length element was used to capture bond slip allowing for accurate strain hysteretic response. In addition, the proposed fiber model has robust dynamic performance although it underestimates the residual displacement by a small amount. The application of this fiber-based modeling technique will be a study of the effect of loading history on the relationship between strain and displacement. By combining finite element modeling with the strain displacement data from the fiber model, characterization of bar buckling will also be possible.

ACKNOWLEDGEMENT

The authors wish to acknowledge Alaska DOT&PF and Alaska University Transportation Centre (AUTC) who supported this research through a series of grants. Special acknowledgement goes to Elmer Marx of Alaska DOT&PF who was closely involved in this research as the primary technical contact. The assistance of the entire staff of the Constructed Facilities Laboratory is appreciated.

REFERENCES

- Goodnight, J. C., Kowalsky, M. J., Nau, J. M. (2012). Experimental Observations on the Effect of Load History on Performance Limit States of Circular Bridge Columns. *15th World Conference on Earthquake Engineering*.
- Filippou, F. C., Popov, E. P. and Bertero, V. V. (1983). Effects of Bond Deterioration on Hysteretic Behavior of Reinforced Concrete Joints. *Report EERC 83-19, Earthquake Engineering Research Center, University of California, Berkeley*.
- Yassin, M. H. M. (1994). Nonlinear Analysis of Prestressed Concrete Structures under Monotonic and Cycling Loads. *PhD dissertation, University of California, Berkeley*.
- Alemdar, B. N. and White, D. W. (2005). Displacement, Flexibility, and Mixed Beam-Column Finite Element Formulations for Distributed Plasticity Analysis. *Journal of Structural Engineering*. **Vol. 131: No. 12**, 1811-1819.
- Neuenhofer, A. and Filippou, F. C. (1998). Geometrically Nonlinear Flexibility-Based Frame Finite Element. *Journal of Structural Engineering*. **Vol. 124: No. 6**, 704-711.
- Scott, M. H. and Fenves, G. L. (2006). Plastic Hinge Integration Methods for Force-Based Beam-Column Elements. *Journal of Structural Engineering*. **Vol. 132: No. 2**, 244-252.
- Zhao, J. and Sritharan, S. (2007). Modeling of Strain Penetration Effects in Fiber-Based Analysis of Reinforced Concrete Structures. *ACI Structural Journal*. **Vol. 104: No. 2**, 133-141.
- Mander, J. B., Priestley, M. J. N. and Park, R. (1988). Theoretical Stress-Strain Model for Confined Concrete. *Journal of Structural Engineering*. **Vol. 114: No. 8**, 1804-1826.
- Paulay, T. and Priestley, M. J. N. (1992). *Seismic design of reinforced concrete and masonry buildings*, Wiley, New York.
- Petrini, L., Maggi, C., Priestley, M. J. N. and Calvi, G. M. (2008). Experimental Verification of Viscous Damping Modeling for Inelastic Time History Analyses. *Journal of Earthquake Engineering*. **Vol. 12:1**, 125-145.
- Pacific Earthquake Engineering Research Center and Network for Earthquake Engineering Simulation (2010). *Website of Concrete Column Blind Prediction Contest 2010*.